Chen *et al. Advances in Bridge Engineering* (2024) 5:6
https://doi.org/10.1186/s43251-024-00117-5

Advances in Bridge Engineering

ORIGINAL INNOVATION

Open Access

Experimental study on long friction-type bolted joint combined with interference fit bolt

Yu Chen[1*], Takashi Yamaguchi[1], Gen Hayashi[1], Motoshi Yamauchi[2] and Keita Ueno[2]

*Correspondence: chenyu@omu.ac.jp

[1] Osaka Metropolitan University, Osaka, Japan
[2] MM Bridge Co., Ltd., Hiroshima, Japan

Abstract

In recent years, high-strength bolts with friction-type joints have been lengthened to withstand increased traffic load. However, with increase in the joint length, the force able to be resisted by bolted joints has decreased owing to uneven distribution of the bolts within the joint. In addition, the proximity of secondary members to the joint has restricted the allowable size of the splice plates. It is therefore necessary to reduce the joint length while maintaining its design strength. In this study, interference fit bolts were assembled at both ends of a friction-type bolted joint to form a hybrid joint, and tensile tests were conducted to elucidate the load transmission mechanism, analyse the slip resistance, and verify whether the addition of the interference fit bolts improves the strength of the friction-type joint. It was concluded that despite a minor slip in the hybrid joint, the slip resistance was approximately 10% higher than that of the friction-type joint, and the overall load–deformation relationship maintained a quasi-linear behaviour up to 1.1 times the slip resistance of the friction-type joint. In addition, the hybrid joint had smaller data scattering than the friction-type joint, suggesting that the uneven load distribution and deformation in the joint was slightly improved by installing the interference fit bolts. The performance of hybrid joints is superior to that of the existing friction-type joints under the current slip limit specification.

Keywords: Bolted joint, Interference fit bolt, Bearing-type connection, Friction-type bolted connection, Long bolted joint, Steel structures, Large scale bridges

1 Introduction

1.1 Background

High-strength bolts (hereinafter referred to as HSBs) are widely used to fasten steel members together as friction-type bolted connections ((hereinafter referred to as friction connection). In recent years, high-strength bolt friction-type joints have become larger, as shown in Fig. 1, to withstand the increased load (Nishimura et al. 2001; JSSC 2013; Wang and Ding 2020). For example, the Minato Bridge in Japan uses bolted joints with 10 rows, and the Jiujiang Yangtze River Bridge in China uses bolted joints with 13 rows. Furthermore, the largest part of the joint in Zhengzhou Yellow River Road-Rail Bridge has 22 rows and 9 columns of bolted joints made with M30 high-strength bolts, and the splice plate has a length of 2100 mm and width of 900 mm (Fei and An 2010).

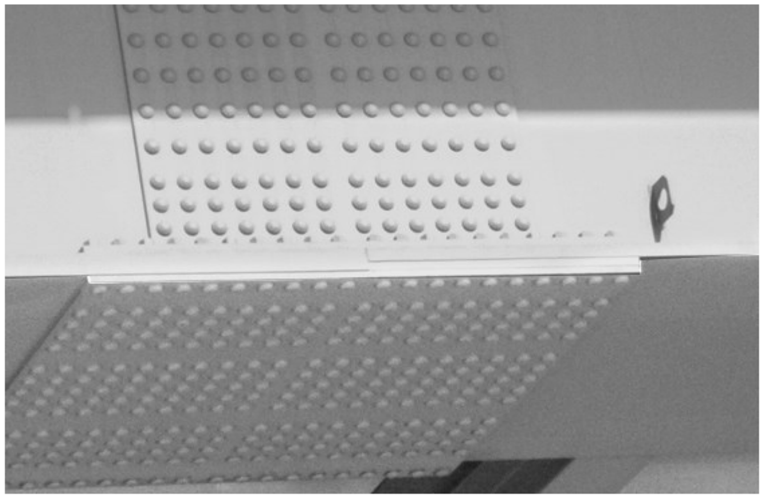

Fig. 1 Long bolted joints at bottom flange

However, the increased joint length of long or large bolted joints has given rise to some problems, such as interference with secondary members in the vicinity of the joint (e.g. stiffener, diaphragm). Moreover, the increased joint length causes uneven distribution of the bolts inside the joint, causing the slip resistance to fall below the designed value (Fisher et al. 1965; Bendigo et al. 1963; Kamei et al. 2000; Chen et al. 2022a, b). Furthermore, owing to the uneven load sharing in the long bolted joint, the bolts do not fracture simultaneously, and the ultimate limit bearing capacity decreases (Takai 2021; Peng et al. 2013; Yamaguchi et al. 2010; Zhao et al. 2022).

Therefore, it is necessary to shorten the joint length without decreasing its strength. For this purpose, it is generally recommended to weld the friction-type bolted joint to shorten the joint length and improve the joint strength. Previous studies (Solodov and Vodyakhin 2022; Manuel and Kulak 2000; Chang and Yeh 2019; Khandel et al. 2022) have demonstrated the reliability and feasibility of welding the friction-type bolted joint during manufacturing (under satisfactory manufacturing conditions). However, the fatigue strength of the weld is lower than that of the friction bolted joint, which directly affects the overall strength of the joint (Manuel and Kulak 2000). Additionally, the environment at the bridge construction site may be too limited to allow welding onsite (e.g. insufficient space or working height constraints). Moreover, welding will destroy the original coating of the steel members. Thus, fabrication of combined welded-bolted connections for steel bridge joints that need to be joined onsite is very difficult. Hence, Suitable methods that can shorten the bolted joint without reducing the strength are required.

1.2 Interference fit bolt

A specialised high-strength bolt for a bearing-type connection (hereinafter referred to as the interference fit bolt) was presented in a previous study (Kulak et al. 2001; Shimozato et al. 2008; Kobelco 2023; Chen et al. 2023). The interference fit bolt possesses the unique feature of an axially ribbed shaft as shown in Fig. 2. Interference fit bolts of B10T grade (courtesy of Kobelco Bolt, Ltd.) used in this study meet the strength requirements

Fig. 2 Interference fit bolt for bearing-type connection (M22, diameter = 23.5 mm, Courtesy of Kobelco Bolt, Ltd.)

of an F10T bolt according to the JIS-B1186 standard (JIS 2018), which is equivalent to ASTM-A490 (ASTM 2014) & Grade 10.9 (ISO 2022). When the bolt is hammered into a hole, the rib undergoes plastic deformation to ensure a tight fit and prevent excessive slipping. Interference fit bolts are employed for retrofitting steel bridge piers with patch plates to address fatigue damage or corrosion (Anami et al. 2019). This is because initial defects or corrosion can cause unevenness of the steel plate surface, making it impossible for the patch plate of the friction-type bolted connection to effectively contact the steel surface and transmit force. However, these bolts are rarely used on other bridge parts owing to their stringent installation requirements.

Regarding bearing-type bolted connections, AASHTO LRFD BDS 2020 (AASHTO 2020) defines a strength limit only for joints subjected to axial compression or joints on bracing members. Both Eurocode3 EN 1993-1-8:2021 (Eurocode3 2021) and GB50017-2017 (GB50017-2017 2017) mention that such connections should be designed in the same way as friction-type bolted connections, and define the serviceability limit state as the slip resistance and bearing resistance as the ultimate limit state. However, Eurocode 3 allows the accumulation of the bearing resistance of resin and slip resistance of injection bolts in the design for the serviceability limit state. Furthermore, Japan Road Association – Japan Specifications for Highway Bridges 2017 - Part II Steel Bridges (JSHB 2017) (hereinafter referred to as JSHB) states that bearing-type bolted connections can be designed to meet the serviceability limit state based on the bearing resistance.

1.3 Objectives

In a previous study (Chen et al. 2023), bearing-type bolts were installed at both ends of the friction-type bolted joint (hereinafter referred to as hybrid bolted joint). The result showed that the 12-row hybrid joint could improve the slip load by approximately 20% when compared with the 12-row friction bolted joint. However, this result was based on numerical analysis and did not consider the actual assembly of the interference fit bolts.

This study focused on interference fit bolts assembled at both ends of a friction-type bolted joint. Tensile tests were performed with three specimens: friction-type bolted joints, hybrid joints, and hybrid joints with interference fit bolts without preloading as shown in Fig. 3. The purpose of this study was to elucidate the load transmission mechanism of the hybrid joints, investigate the slip resistance, and verify the utility of installing interference fit bolts in friction type joints to improve joint strength.

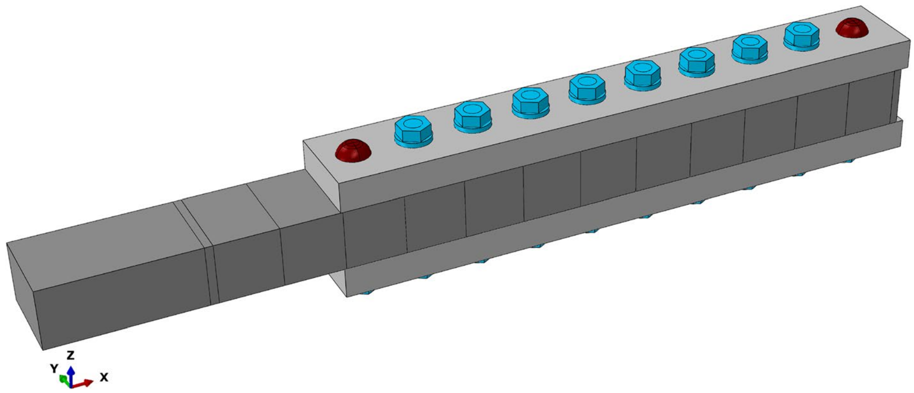

Fig. 3 Schematic of hybrid joint (combination of friction-type and bearing-type bolted connections)

Table 1 Material test results

Component name	Plate 28 mm		Plate 50 mm		Interference fit bolt (B10T)	High-strength bolt (F10T)	
	Inspection Certificate	Test Result	Inspection Certificate	Test Result	Inspection Certificate	Inspection Certificate	Test Result
Yield Strength $[N/mm^2]$	536	525.5	549	548.6	1025	998	1087
Ultimate Strength $[N/mm^2]$	633	619.5	646	635.5	1073	1075	1194
Young's modulus E $[kN/mm^2]$	-	209	-	213	-	-	204
Poisson's ratio v	-	0.274	-	0.269	-	-	-
Elongation [%]	26	-	46	-	19	19	-

2 Experiment

2.1 Material test

The material test specimens were prepared in accordance with JIS Z 2241 2011 (JIS 2011). Material tests were conducted on three steel specimens with thicknesses of 50 mm and 28 mm. The results are summarised in Table 1.

2.2 Slip coefficient test

The slip coefficient test was conducted with the same surface condition as in the slip test, the geometry of the standard slip test specimen is shown in Fig. 4, and the structural characteristics are shown in Table 2. The geometry was prepared with reference to the high-strength bolt design, construction, and maintenance guidelines (JSCE 2014).

where, t_m is the thickness of main plate, t_s is the thickness of splice plate, w is the width of mian plate, e_1 is the end distance from bolt hole, p_1 is the bolt spacing.

The result of slip coefficient test as shown in Table 3, the average of slip coefficient μ is 0.804, both the bolt preload and the slip coefficient have a low variation.

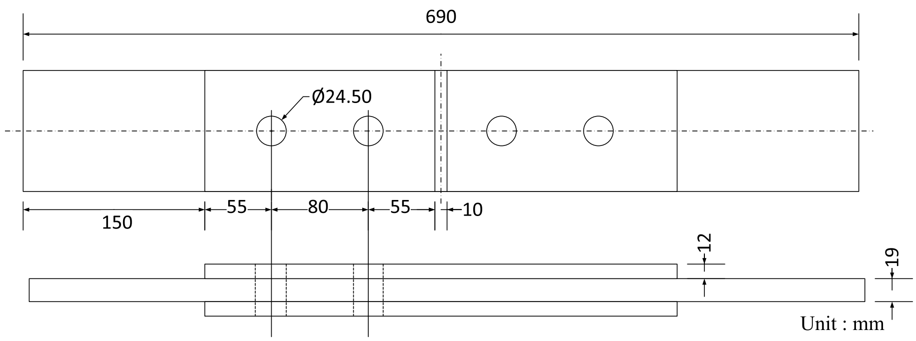

Fig. 4 Geometry of slip coefficient test specimens

Table 2 Shape of standard slip specimen

Bolt grade	***d***	d_0	**Steel grade**	f_y	t_m	t_s	***w***	e_1	p_1
F10T	22	24.5	SM490Y	355	19	12	100	55	80

Table 3 Result of slip coefficient test

Name	**Preload**		**Slip load**	**Slip Coefficient**
	Before loading	**Avg.**		
test-1	108.58	105.6	332.2	0.786
	102.74			
test-2	107.18	107.6	352.4	0.819
	108.42			
test-3	107.18	107.8	348.4	0.808
	108.42			
Mean				0.804
Standard Deviation				0.017

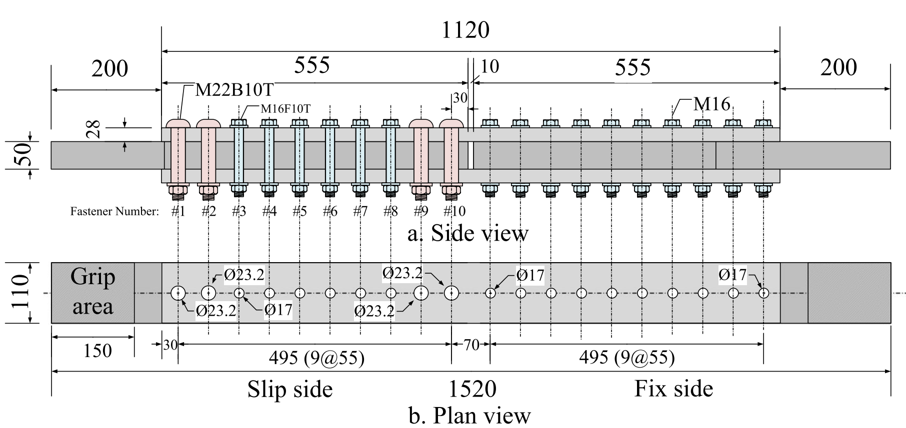

Fig. 5 Detailed dimensions of hybrid joint (Unit: mm)

2.3 Experimental details for hybrid joint

The specimen dimensions shown in Fig. 5 were selected based on previous research (Kamei et al. 2000) on an actual bridge. The commonly occurring single-row 10-column arrangement was used as the reference. To investigate the mechanical behaviours of the slip and bearing of the joints, the ratio between slip resistance and net cross-section yield resistance β was set to 0.65 to prevent the joints from being affected by the cross-sectional yield of the main plate before slippage.

The specimens were subjected to loading using a hydraulic universal testing machine with a capacity of 2000 kN (provided by Tokyo Testing Machine Co., Ltd.). Considering the loading capacity of the testing machine, the specimen was scaled down to a size of 16/22. Static uniaxial tension testing was conducted. The loading rate was set to 1 kN/s until either the test machine capacity was reached or failure occurred in the net cross section of the plate or shear area of the bolt. The loading device is depicted in Fig. 6.

Figure 7 shows the measurement locations for the relative displacement, joint deformation, and strain. Clip displacement gauges were used to measure the relative displacement. The joint deformation was measured using a linear variable differential transformer (LVDT). The strain was measured using a strain gauge and a camera. Additionally, random patterns were applied to side-2 of the joint to capture the strain and displacement on the lateral side of the joint using the digital image correlation (DIC) method.

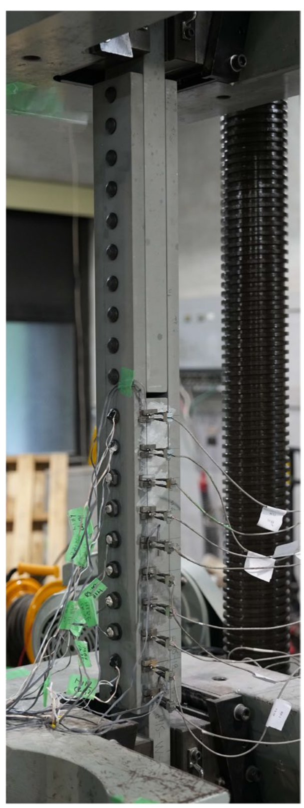

Fig. 6 Experimental setup

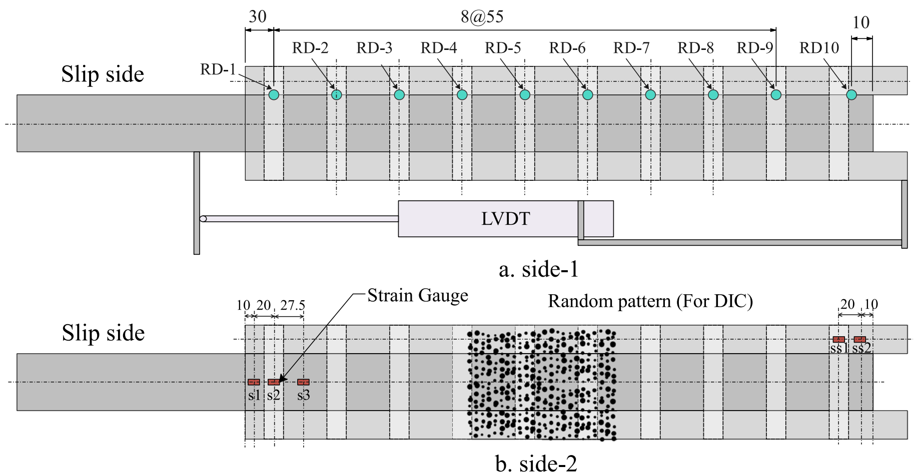

Fig. 7 Measurement locations (Unit: mm)

Table 4 Experimental specimens

Specimens	Fastener number (slip side)										Bolt Preload [kN]
	#1	#2	#3	#4	#5	#6	#7	#8	#9	#10	
Friction	○	○	○	○	○	○	○	○	○	○	117
Hybrid	✿	✿	○	○	○	○	○	○	✿	✿	117
Hybrid-NAF	✿	✿	○	○	○	○	○	○	✿	✿	○: 117, ✿: 5 – 10

○: High-strength bolt, ✿: Interference fit bolt

According to JSHB (2017), the joint surface was coated with inorganic zinc-rich paint with a presumed slip coefficient of 0.8, as determined from the slip factor test on two bolts with the same plate thickness and same faying surface condition as used in this test.

Since the smallest diameter of interference fit bolts currently produced in Japan is M22, M22 interference fit bolts were used in our specimens. Considering that the net cross–sectional yield resistance (for M16: 2580 kN, M22: 2374 kN) greatly exceeds the slip resistance (1696 kN), the influence of increased bolt holes on slip resistance is practically negligible.

Interference fit bolts were installed using holes with diameters of 23.2 mm. According to AASHTO (2020), the common M16F10T bolt is installed using a 17 mm-diameter hole. Taking relaxation into account, the preload during the installation of all bolts was 117 kN (JSHB 2017). Strain gauges were used to measure the bolt preload, and the relationship between strain and bolt preload was determined through a calibration test.

2.4 Experimental cases

The experimental specimens are shown in Table 4. Previous research (Chen et al. 2023) found that for long bolted joints with a single column of 8–12 rows, at least two or more interference fit bolts should be used at each end of the joint to prevent excessive load sharing and premature shear yield of the bolts. Moreover, during the tightening process of the bolts, the bolt shank may undergo shrinkage caused by the Poisson effect, potentially leading to reduced effectiveness of the interference fit. Therefore, in this experiment, the hybrid case employed two interference fit bolts at each end, whereas the hybrid-NAF case did not apply a preload for the interference fit bolt, which was tightened to only 5–10 kN using a ratchet.

Three groups of specimens (one group have three cases: friction, hybrid, hybrid-NAF) were used for testing in this study. The specimens in the same group were controlled to identical environmental conditions, relaxation time, and preload as possible. where, the other group did not obtain valid results because the experiment failed and was therefore excluded from the comparison.

3 Experimental results

3.1 Installation of interference fit bolt

According to the regulations of the JSHB (2017), the precision requirement for the bolt hole corresponding to the M22 bolt in bearing-type connections is 23.5 ± 0.3 mm. However, the maximum measured outer diameter of the interference fit bolt shaft was 23.6 mm. To confirm the effectiveness of the interference fit with the bolt hole after the installation, specimens with bolt hole diameters of 23.6 mm, 23.5 mm, and 23.2 mm were produced. Five interference fit bolts were randomly selected, and the average maximum outer diameter of the bolt shaft (including the rib), measured using a vernier calliper, was $23.5 + 0.1$ mm.

The hole creation method involved drilling a pilot hole that was 1 mm smaller than the target diameter, followed by enlarging the hole to the target diameter using a reamer. This approach guaranteed accuracy of the bolt hole diameter to within $\pm$ 0.02 mm.

The results showed that when the bolt hole was 23.6 mm, the bolt could easily pass through the hole without achieving an interference fit. When the bolt hole was 23.5 mm, it was not possible to insert the bolt into the hole by hand, but a hammer could be used with less force to install the bolt into the hole. When the bolt hole was 23.2 mm, a significant amount of force was required to hammer the bolt into the hole.

Figure 8 shows the cross sections of the bolt and test plate. In both the 23.5 mm- and 23.2 mm-diameter holes, it can be observed that the ribs of the bolt have undergone plastic deformation, resulting in an interference fit. Figure 8 reveals that the degree of deformation is more significant in the bolt shaft ribs and hole wall of the test piece with the 23.2 mm-diameter hole. To achieve a better interference fit for the bolt, the diameter of the bolt hole for the interference fit bolt used in this experiment was set to 23.2 mm.

3.2 Deformation and relative displacement

Figure 9a shows the relationship between the load and overall deformation of the joint. Figure 9b illustrates the results of two groups, which demonstrated nearly identical behavior in two experiment groups. Table 5 summarizes the slip load for both groups. The average slip load for the friction type joint is 1380 kN, with a difference of 2.6% between the two groups. For the hybrid joint, the average slip load is 1473 kN, with a difference of 2.3% between the two groups. The average slip load for the hybrid-NAF joint is 1213 kN, with a difference of 4.2% between the two groups.

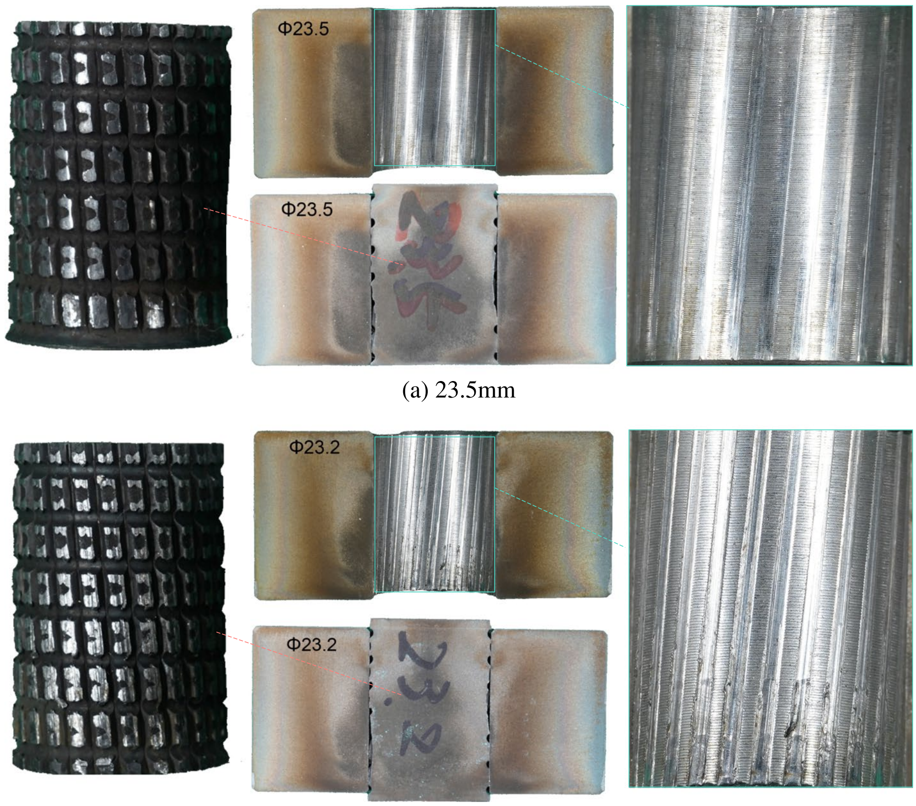

(a) 23.5mm

(b) 23.2mm

Fig. 8 The bearing status of the bolt shank and bolt hole

These differences in slip load can be attributed to variations in construction conditions. Since there is a small difference between the two groups of specimens, it could be considered that the mechanical behavior of the same type of specimens will not change significantly under the same construction conditions, such as having the same surface condition and the bolt preload. To ensure accurate comparisons and minimize experimental errors, this discussion will focus on analyzing one group of specimens. These specimens were tested on the same day, under nearly identical construction conditions, and with minimal variation in bolt preload.

Slippage was observed at the friction-type joint at 1361 kN, with the load decreasing to approximately 1048 kN (a change rate of approximately 23%). The overall deformation of the joint increased from 3.7 mm to 6.5 mm (a change rate of approximately 75%). For the hybrid joint, slippage occurred when the load reached 1456 kN, and the load decreased from 1456 to 1407 kN (a change rate of approximately 3%). The joint deformation decreased from 3.955 mm to 3.989 mm (a change rate of only approximately 0.8%). The overall load–deformation relationship of the hybrid joint remained quasi-linear K_0 up to the upper load limit of 1800 kN, notwithstanding a small amount of slip, and the residual deformation was only 1 mm. In addition, a comparison of the hybrid-NAF case with the hybrid case shows that besides a slight decrease in the initial slope and a minor reduction in the slippage load, the trends of the curve were not significantly different.

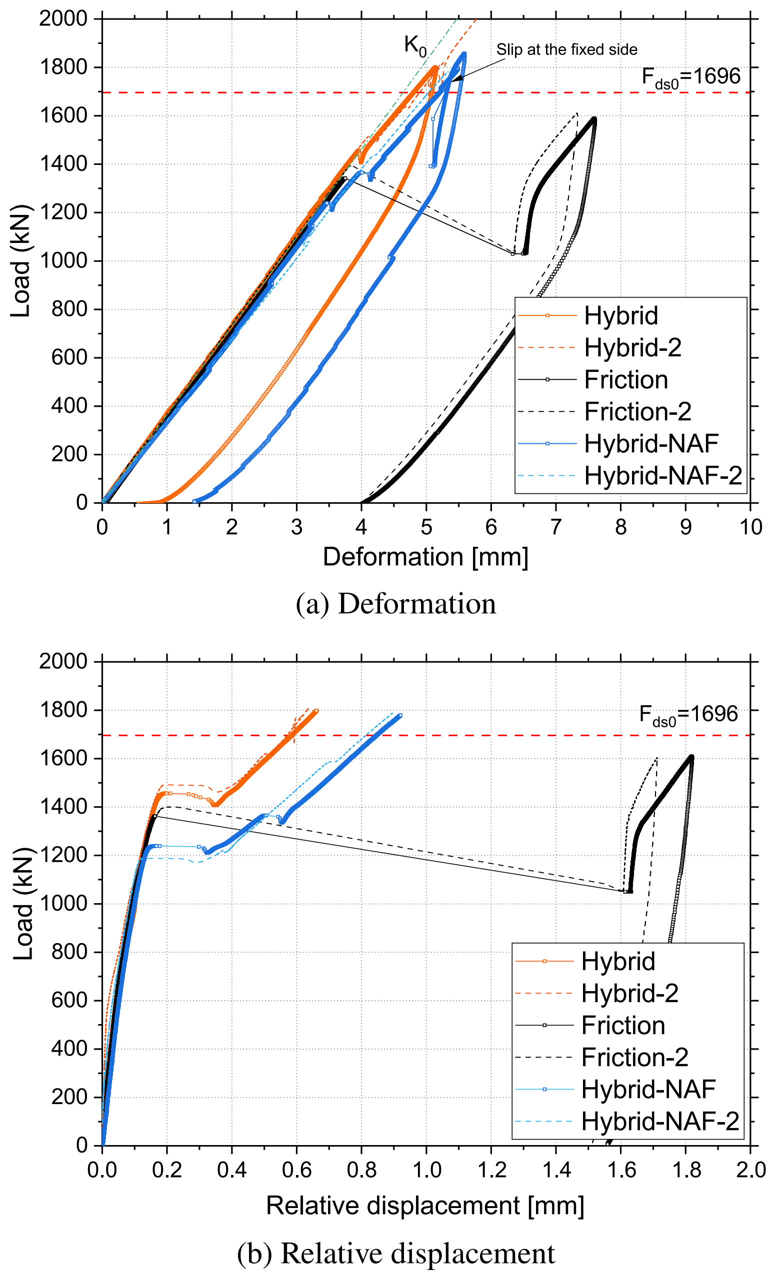

Fig. 9 Relationship between load and deformation or relative displacement

Table 5 Result of slip load

	Friction		Hybrid		Hybrid-NAF	
	1	**2**	**1**	**2**	**1**	**2**
Slip load [kN]	1362	1398	1456	1491	1239	1188
Mean [kN]	1380		1473.5		1213.5	
Diff. (for two group) [%]	2.6		2.3		4.2	

Figure 9b shows the relationship between load and relative displacement at a distance of 10 mm from the end of the main plate (RD-10). Similar to the overall deformation, significant slippage occurred at the friction-type joint, with relative displacement increasing from 0.163 mm to 1.632 mm (an increase of approximately 901%). In the hybrid joint, the relative displacement increased from 0.184 mm to 0.342 mm (an increase of approximately 85%). The hybrid joint exhibited a small amount of slippage, as observed in the results of previous studies (Kamei and Taniguchi 2010) on individual interference fit bolts. This was attributed to a small clearance between the bolt hole wall and rib of the interference fit bolt, resulting in inevitable slight slippage. The slip load of the hybrid joint was 7% higher than that of the friction-type joint. The slip load reduction and slippage are summarised in Table 6.

3.3 Bolt preload

Figure 10 shows the relationship between the bolt preload reduction ratio and load of each bolt. The bolt preload reduction ratio was calculated as N/N_0, where N is the real-time bolt preload and N_0 is the bolt preload before loading.

For the friction-type joint, the most significant decrease in the bolt preload occurred on bolt #10, where the preload dropped to approximately 90% when slip occurred (1362 kN), as shown in Fig. 10a. This is a 5% difference when compared with the value for bolt #6, which had the smallest decrease in the preload. The significant reduction in the preload at bolt #10 was attributed to the deformation of the splice plate, which was greater than that of the main plate at bolt #1. Although the main plate had a larger net cross section than the splice plate, considering the stress enhancement of 1.1 times due to friction on the net cross section of the main plate, the stress at the net cross section of the splice plate would be almost the same as that on the main plate when subjected to the same tension. Moreover, it was found that the strain at bolt #10 of the splice plate was greater than the strain at bolt #1 of the main plate. Furthermore, excepting bolt #1, the preload of the other bolts did not decrease uniformly, showing an approximate variation of 2%. At the load of 1362 kN, a severe impact occurred due to the large slip in the joint and momentary transition of the joint from a sliding to a bearing state.

Table 6 Summary of load drop and slip deformation

Case	Slip Begins	End of Slip	Difference	Rate of Change
Load [kN]				
Friction	1362	1048	-313	-23%
Hybrid	1456	1407	-49	-3%
Hybrid-NAF	1239	1210	-28	-2.2%
Deformation [mm]				
Friction	3.7	6.5	2.8	+75%
Hybrid	3.955	3.989	0.034	+0.8%
Hybrid-NAF	3.46	3.54	0.08	+2.3%
Relative Displacement [mm]				
Friction	0.163	1.632	1.469	+901%
Hybrid	0.184	0.342	0.158	+85%
Hybrid-NAF	0.146	0.327	0.181	+124%

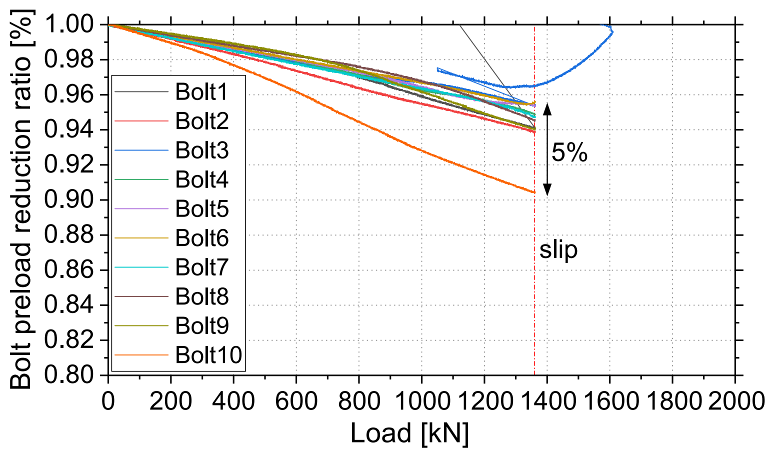

(a) Friction-type joint

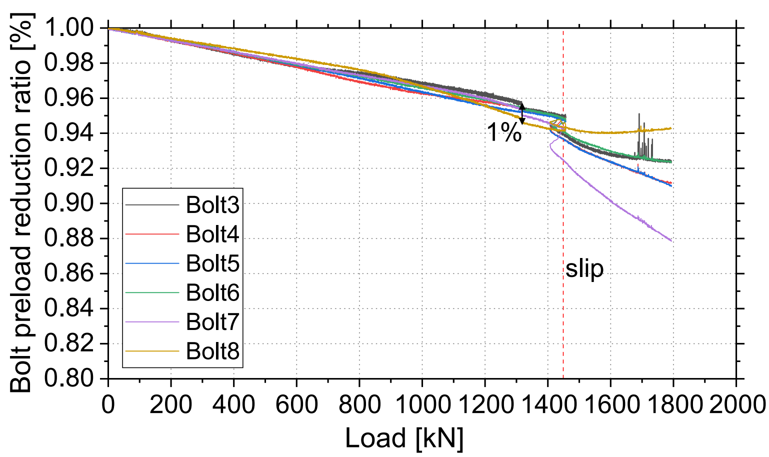

(b) Hybrid joint

Fig. 10 Relationship between bolt preload reduction ratio and load of each bolt

Consequently, all strain gauges on the bolts were damaged and it was not possible to obtain the bolt preload data.

At the load of 1362 kN on the hybrid joint shown in Fig. 10b, the bolt reduction ratio was uniformly distributed with a variation of approximately 1% when compared with the result for the friction-type joint. Although we did not measure the preload for the interference fit bolt, based on the data from HSB (i.e. bolt # 3 – # 8), we posit that the load distribution of the hybrid joint was more uniform than that of the friction-type joint. Moreover, the variance in the preload of each bolt under slippage was not significant, even at 1456 kN. When the load reached 1800 kN, the maximum reduction ratio in the preload variation was only 6%. Therefore, it can be considered that the load distribution of hybrid joints is more uniform and load transmission is smoother when compared with those of friction-type joints.

3.4 Distribution of relative displacement

The distribution of the relative displacement (for load $= 0.8F_{sf} = 1088$ kN, where F_{sf} is friction-type joint slip load) is shown in Fig. 11. The green bar represents the

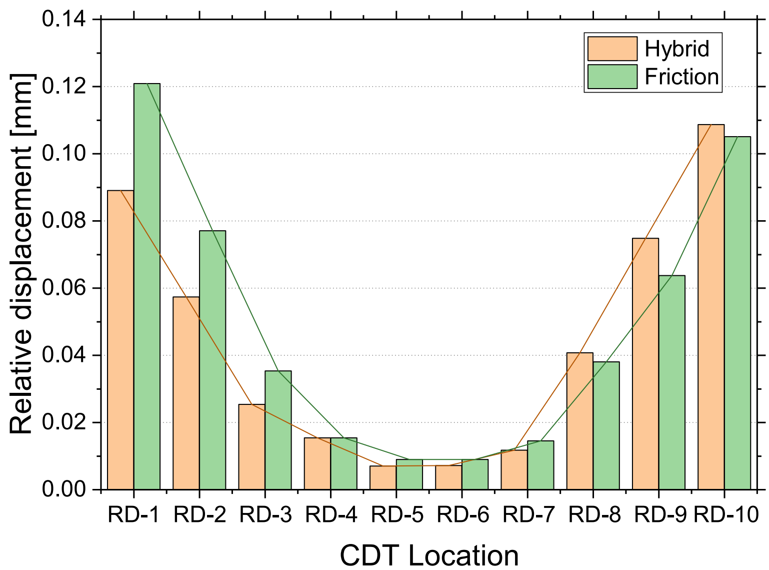

Fig. 11 Distribution of relative displacement (when load = $0.8F_{sf}$ = 1088 kN, where F_{sf} is friction-type joint slip load)

friction-type joint and orange bar represents the hybrid joint. For the positions RD-1 and RD-2 at the ends of the joint, the relative displacement of the hybrid joint was significantly lower than that of the friction-type joint. This low relative displacement can be attributed to the interference fit of the bolts # 1 and # 2, making it more difficult to generate the relative displacement when the elastic slip stage is nearing completion. However, at the other end of the hybrid joint, in interference fit bolts # 9 and # 10, the relative displacements at RD-8, 9, and 10 were actually higher than those of the friction-type joint. It is speculated that the higher relative displacement observed at bolts #9 and #10 are due to a suboptimal interference fit.

In addition, the hybrid joint has a more uniform distribution of relative displacement when compared with the friction-type joint. This finding is consistent with the results discussed in Section 3.3 regarding the distribution of bolt preload reduction. Thus, it can be inferred that the hybrid joint demonstrates a more uniform load distribution mechanism. The load sharing mechanism discussed in this paper is similar to the analytical discussions found in previous studies (Chen et al. 2023).

4 Discussion

4.1 Cross-section observation after slipping

Figure 12 shows the cross section of the hybrid joint subjected to a load of up to 1800 kN. Figure 12a shows the cross-sectional diagram of the bolts #1 – # 3. The figure reveals that the deformation of the rib on the non-bearing side is very small, as observed in the magnified portion of bolt #1 on the right side. Likewise, the magnified section of Bolt #2 on the opposite side of the bearing suggests minor deformation of the rib. It appears that some ribs do not contact the hole wall when the interference fit bolt is hammered into the hole. Consequently, the desired interference fit is not produced, resulting in a minor slip in the joint. This slip is believed to be caused by

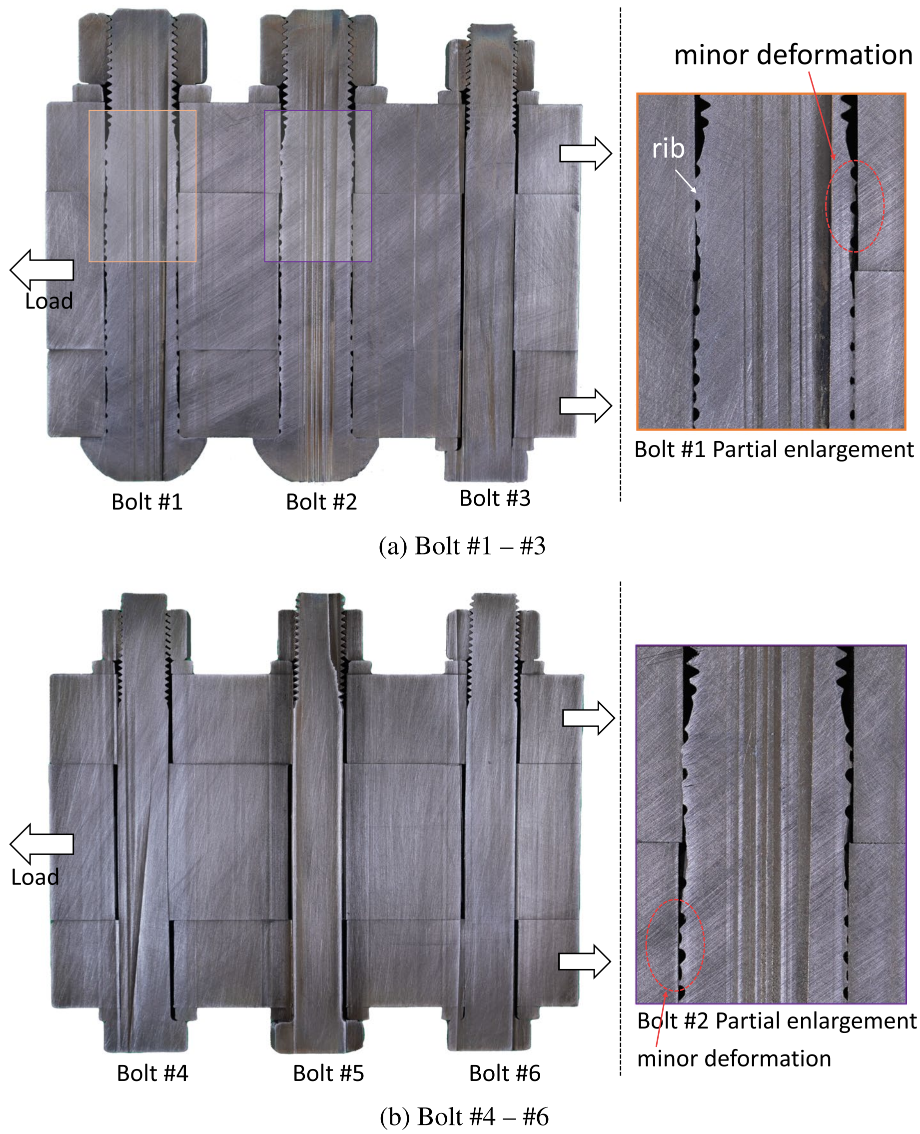

Fig. 12 Cross sections of each bolt of the hybrid joint under loading of up to 1800 kN

the clearance created during the bolt installation as well as the small plastic deformation of the rib.

Figure 13 shows the displacement at the side of the hybrid joint under a load of 200 kN, measured using the DIC method. It was found that the displacement on the nut side of the joint (i.e. SP2 side) was greater than that on the bolt head side (i.e. SP1 side). This observation is consistent with the results obtained from the cross-sectional observations. Insufficient interference fit increased the displacement and caused slight slippage.

4.2 Load reduction for long bolted joint

The European Convention for Constructional Steelwork (ECCS), ISO/TC and Eurocode 3 (EN 1993-1-8:2021) (ECCS 1985; ISO 1997; Eurocode3 2021) specify that the resistance should be reduced by a factor of when the spacing between the first and last bolts

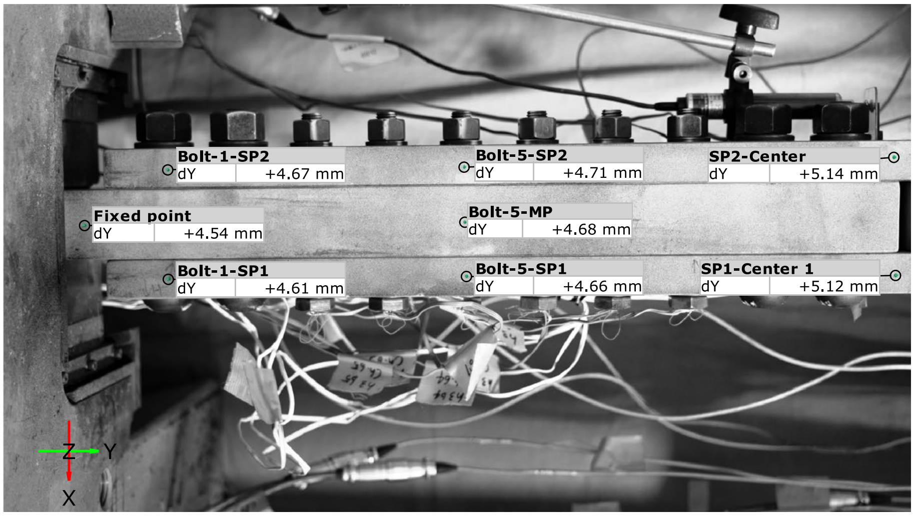

Fig. 13 Displacements of hybrid joint under the load of 200 kN

Table 7 Slip resistance reduction ratio for each case examined in this study

	Slip load P_s kN	Slip resistance F_{ds} kN	Load reduction rate
Hybrid	1456	1618	0.90
Hybrid-NAF	1239	1341	0.91
Friction	1362	1726	0.79

in a joint is larger than 15d. AASHTO (2020) specifies that the nominal shear resistance of bolts in joints longer than 38.0 in. must be reduced by an additional factor of 0.83 or 0.75/0.9.

Furthermore, owing to the non-uniformity of the load distribution, the bolts do not fracture simultaneously, leading to a reduction in the ultimate limit bearing capacity (Takai 2021; Peng et al. 2013; Yamaguchi et al. 2010).

Table 7 presents the experimentally acquired slip loads P_s for each case along with their corresponding calculated slip resistances F_{ds}. It also shows the load reduction rate between the experimentally acquired slip loads P_s and the calculated values F_{ds}. Eurocode 3 (2021) recommends that interference fit bolts should be designed by calculating the slip resistance in the same way as followed for the HSB friction-type connection. The slip resistance F_{ds} was calculated from Eq. 1, and slip load P_s denotes the load when the first load drop occurred. The lengths of the friction and hybrid joints, L_j, were both 495 mm (where L_j is the distance between the centres of the end fasteners in a joint). The load reduction rate of the friction-type joint reached 0.79, which was lower than the values specified by Eurocode 3 (calculated to be 0.92) and JSHB (calculated to be 0.96). This was attributed to the use of a thick plate (50 mm for the main plate) in this experiment. Because the thick plate causes the bearing stress on the bolt to be uneven, the bolt will be more susceptible to bending deformation, resulting in loss of preload. The hybrid joints had a slip load reduction of 0.9, which was approximately 10% higher than that of friction-type joints. The slip resistance reduction ratio for the hybrid joint without preload (hybrid-NAF case) on the interference fit bolts was 0.92, which approximately matched that of the hybrid joint. This was because regardless of the presence of preload on the interference fit bolt, the extent of slip until increase in load was nearly the same in both cases, and depends on the gap between the bolt and hole wall and plastic deformation of the rib.

$$F_{ds} = \sum_{n} \mu \times N_0 \times m, \tag{1}$$

where μ is the slip coefficient ($=0.8$) determined from the slip factor test in which two bolts were used and the plate thickness and faying surface condition were the same as used in this test (see Section 2.2). N_0 is the preload on the bolts before loading, m is the number of shear planes, and n is the number of the bolt.

In addition, theoretical calculations indicated that applying a preload of 106 kN to a bolt with a diameter of 22 mm would result in a contraction of 0.009 mm, which is much smaller than the manufacturing tolerance of the bolt hole or bolt shank diameter. Therefore, the horizontal shrinkage of the bolt shaft was small enough to be considered negligible.

The bolt shaft shrinking value (Δd) is

$$\Delta d = \delta_{yb} d_{ib} = \frac{N_0 \nu}{EA} d, \tag{2}$$

where δ_{yb} is the bolt strain in the y-direction (axial direction), d_{ib} is the diameter of the interference fit bolt, and A_{ib} is the cross-sectional area of the interference fit bolt shaft.

Therefore, the quantity of bolt preload does not have a significant effect on the slip behaviour. In addition, it can be inferred that the reduction in slip load is related to the bearing capacity of the rib, as insufficient contact area of the rib results in excessive contact pressure and compression plastic deformation.

Figure 14 shows the relationship between the normalised load and normalised deformation. Comparison of the hybrid joint with the friction-type joint indicates a higher initial slope for the former, which exhibits quasi-linear behavior despite minor slip. Insufficient interference fit causes this minor slip, leading to the interference fit bolt's inability to fully resist the portion of the load lost due to slip. Even when loaded to 1.1 times the slip resistance F_{ds}, and subsequently unloaded, there was only a residual deformation of 0.2% relative to the length of the joint.

4.3 Limit state

A previous study (Fisher et al. 1965) showed that load is first transmitted by the connection with higher stiffness, and the bearing-type connection will play a significant role in load sharing only when the friction-type connection approaches its limit. Therefore, the limit state of a hybrid joint relies on the state of the bearing-type connection, which can manifest as either the shear yield limit of the bolt or bearing deformation limit of the main plate.

This study considered that for hybrid joints that use both bearing-type bolted connections and friction connections, the design under the serviceability limit state can be

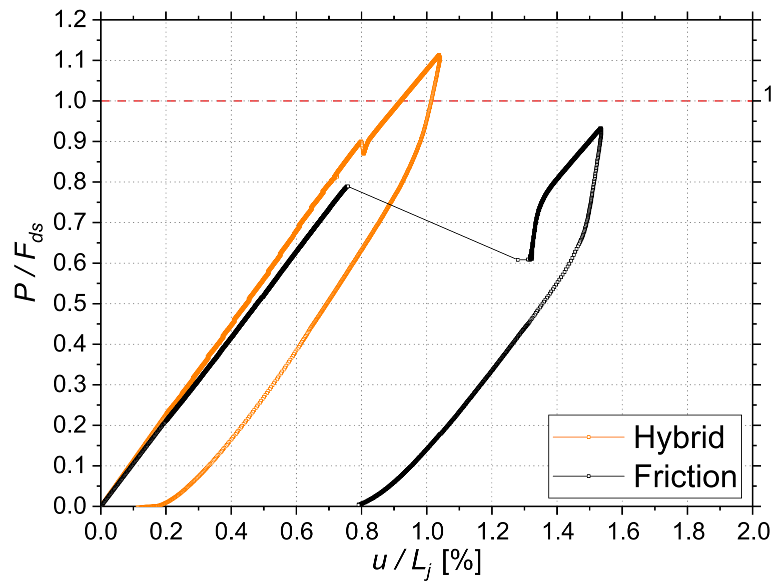

Fig. 14 Relationship between normalised load and normalised deformation. (Normalised load is the load divided by the slip resistance F_{ds}, and normalised deformation is the deformation divided by the joint length L_j)

performed by accumulating the bearing resistance of the interference fit bolt and slip resistance of the HSB.

However, in this experiment, slight slippage occurred in the hybrid joint, which was believed to be caused by the gap between the rib and hole wall. Therefore, regarding the limit state of the hybrid joint, in reference to the Japanese AIJ recommendations for Design of Connections in Steel Structures (AIJ 2012) a slip limit of 0.2 mm can be defined. The maximum load for a relative slip coefficient of 0.2 mm was taken as the serviceability limit state, which is the slip resistance F_{ds} in Table 7. Because a slight slip occurred in the hybrid joint in this experiment, the behaviour after 0.2 mm could not be determined based on these data.

Despite this, hybrid joints in the slip limit state exhibit greater strength when compared with friction-type joints. The load distribution is also more even and the relative displacement of the ends is smaller. In addition, the hybrid joint remained quasi-linear up to the upper load limit of 1800 kN. Hence, the performance of hybrid joints is superior to that of the existing friction-type joints under the current slip limit specification.

5 Conclusions

This study focuses on interference fit bolts assembled at both ends of 10-row friction-type bolted joint to elucidate the slip resistance and deformation of the hybrid joints, and to verify whether the interference fit bolts can be assembled in the friction-type joints to improve the strength of the joint. Tensile tests were performed with three specimens: friction-type bolted joint, hybrid joint, and hybrid joint with non-preload interference fit bolts.

On the basis of the results for the10-row hybrid bolted joint, we arrive at the following findings and conclusions.

1. The slip load of the 10-row hybrid joint assembled with four interference fit bolts at both ends is approximately 7% higher than that of a friction-type joint. If the initial preload of the bolts is considered inconsistent, the result of dividing the slip load by the corresponding calculated slip resistance is approximately 10% higher for the hybrid joint than that for the friction-type joint.
2. The distributions of relative displacements and reduction in preload on the individual bolts of the joint show that the hybrid joint has small dispersion of data when compared with the friction-type joint, suggesting that uneven load distribution and deformation of the joint is improved by installing interference fit bolts. This allows the inner bolts of the hybrid joint to share a greater part of the load than the friction-type joint for the same load level, thus reducing the load concentration on the outer bolts. The deformation of the hybrid joint improves owing to the considerable reduction in the outermost relative displacement RD1. The performance of hybrid joints is superior to that of the existing friction-type joints under the current slip limit specification.
3. The overall load–deformation relationship of the hybrid joint remains quasi-linear up to the upper load limit of 1800 kN, although a minor amount of slip occurs. Moreover, the total residual deformation of the hybrid joint is only 0.2% relative to the length L_j of the joint. In contrast, the friction-type bolted joint produces a residual deformation of 0.75% when loaded to 1600 kN. Therefore, within the quasi-linear range, it can be expected that the hybrid joint will have a high serviceability limit strength.
4. Observation of the cross section showed that the rib portion of the interference fit bolt tail did not provide a good interference fit (the rib was not in contact with the hole wall or the contact area was too small). This resulted in the interference fit bolt being unable to fully resist the portion of load lost due to the slip, causing a minor slip to occur. This is also illustrated by the fact that the displacement of the splice plate SP2 on the nut side is greater than that of the splice plate SP1 on the head side of the bolt.

Future studies will address the bearing limit state for hybrid joints and present a practical equation for determining their bearing resistance.

Acknowledgements

The authors would like to acknowledge the members of the Bridge Engineering Lab. of Osaka Metropolitan University for their help and support of this experiment, and Masayori Yoshimi of Nippon Steel Bolten Co. for his advice on bearing type bolts. We would like to thank Editage (www.editage.jp) for English language editing.

Authors' contributions

Yu Chen: Conceptualisation, Investigation, Methodology, Writing - original draft. Takashi Yamaguchi: Supervision, Resources, Methodology, Writing - review. Gen Hayashi: Methodology, Writing - review. Motoshi Yamauchi: Resources, Methodology, Writing - Review. Keita Ueno: Resources, Methodology, Writing - review.

Funding

This work was supported by the SPRING program of the Japan Science and Technology Agency (JST SPRING) [grant number JPMJSP2139].

Availability of data and materials

Partial data supporting the findings of this study are available upon request from the corresponding author.

Declarations

Competing interests
The authors declare that they have no competing interests.

Received: 4 December 2023 Accepted: 3 February 2024
Published online: 01 March 2024

References
AASHTO (2020) AASHTO LRFD Bridge Design Specifications, 9th edn. American Association of State Highway and Transportation Officials, Washington, DC
AIJ (2012) AIJ Recommendations for Design of Connections in Steel Structures. Architectural Institute of Japan, Tokyo
Anami K, Takebuchi T, Yoneyama T et al (2019) Repair with splice plate for fatigue crack at vertical stiffener of orthotropic steel deck using bearing type bolt. J Struct Eng (JSCE) 65A:533–543
ASTM (2014) Standard Specification for Structural Bolts, Alloy Steel, Heat Treated, 150 ksi Minimum Tensile Strength. American Society for Testing and Materials International, West Conshohocken
Bendigo RA, Hansen RM, Rumpf JL (1963) Long bolted joints. J Struct Div 89(6):187–213
Chang HY, Yeh CY (2019) A study on behavior of steel joints that combine high-strength bolts and fillet welds. Steel Compos Struct 31(4):361–372. https://doi.org/10.12989/scs.2019.31.4.361
Chen Y, Sakura R, Yamaguchi T et al (2022a) Load transferring mechanism of long riveted joint partially replaced by high-strength bolts. IABSE Symp Prague 2022:173–180. https://doi.org/10.2749/prague.2022.0173. https://structurae.net/en/literature/id/10676406
Chen Y, Yamaguchi T, Yamauchi M, et al (2022b) Study on the mechanism of load transferring of riveted joints with high strengh bolts as frictional joints. J Steel Constr Eng (Jpn) 29:1–14. https://doi.org/10.11273/jssc.29.113_1
Chen Y, Yamaguchi T, Hayashi G et al (2023) Mechanical behavior of hybrid joint with bearing-type and slip-critical bolted connections. J Constr Steel Res 211:108172. https://doi.org/10.1016/J.JCSR.2023.108172
ECCS (1985) European Recommendations for Bolted Connections in Structural Steelwork, 4th edn. ECCS Technical Committee 10 Bolted and Welded Connections, Brussels
Eurocode3 (2021) EN 1993-1-8: Eurocode 3: design of steel structures - Part 1-8: Design of joints. European Committee for Standardization, London
Fei C, An Y (2010) Quality control in tightening construction of high strength bolts in highway-railway bridge over yellow river at zhengzhou. Railw Standard Des (Chin) 9:82–85
Fisher J, Kulak G, Beedle L (1965) Behavior of Large Bolted Joints, issue no 7. Fritz Laboratory Reports, Washington, D.C.
GB50017-2017 (2017) Code for design of steel structures (English Version). China Architecture & Building Press, Beijing
ISO (2022) ISO 4014: Fasteners - Hexagon head bolts - Product grades A and B. International Organization for Standardization, Geneva
ISO I (1997) ISO 10721-1:1997 Steel structures - Part 1: Materials and design. ISO/TC 167/SC1 Steel: Material and design, Geneva
JIS (2011) JIS Z 2241-2011: Test pieces for tensile test for metallic materials. Japan Insustrial Standards Committe, Tokyo
JIS (2018) JIS B 1186: Sets of high strength hexagon bolt, hexagon nut and plain washers for friction grip joints, 13th edn. Japan Insustrial Standards Committe
JSCE (2014) Japan Society of Civil Engineers - Design Code for Steel Structures Part A: Structures in General. Japan Road Association, Tokyo
JSHB (2017) Japan Specifications for highway bridges - Part 2 Steel Bridges and Members. Japan Road Association, Tokyo
JSSC (2013) Current technology and expectations of high strength bolted joints, JSSC technical report. 96, Japanese Society of Steel Construction
Kamei Y, Taniguchi Y (2010) An analytical study on the load transmission mechanism and the limit state of bearing connection with high strength bolts. Steel Constr Eng (Japanses) 17:45–54. https://doi.org/10.11273/jssc.17.68_45
Kamei Y, Matsuno M, Nishimura N (2000) An Analytical study on slip strength of multi HSFG bolted joints in tention. J Jpn Soc Civ Eng Ser A1 (Jpn) (640):49–60. https://doi.org/10.2208/jscej.2000.640_49
Khandel O, Tamimi MF, Soliman M et al (2022) Reliability assessment of connections with slip-critical bolts and fillet welds in combination. J Constr Steel Res 188:107036. https://doi.org/10.1016/j.jcsr.2021.107036
Kobelco (2023) High strength bolt for bearing type connection. https://www.shinkobolt.co.jp/products-english/. Accessed 08 Aug 2023
Kulak GL, Fisher JW, Struik JH (2001) Guide to design criteria for bolted and riveted joints, 2nd edn. American Institute of Steel Construction. https://doi.org/10.1139/l88-018
Manuel TJ, Kulak GL (2000) Strength of joints that combine bolts and welds. J Struct Eng 126(3):279–287. https://doi.org/10.1061/(ASCE)0733-9445(2000)126:3(279)
Nishimura N, Akiyama H, Kamei Y (2001) Trend of studies on high-strength friction grip bolt joint. J Jpn Soc Civil Eng (Jpn) 1–14. https://doi.org/10.2208/jscej.2001.675_1
Peng X, Ymaguchi T, Takai T et al (2013) Fea study on the slip behavior of high strength multi bolted friction type joints with thick plates by structural dimensions. J Jpn Soc Civ Eng Ser A1 (Jpn) 69:452–466
Shimozato T, Kinomoto T, Miki C (2008) Experrimental study on behaviors of bearing type bolts and fem analysis model. J Jpn Soc Civ Eng (Jpn) 64:167–178
Solodov NV, Vodyakhin NV (2022) Experimental study and computer simulatio236122223n of the work of combined bolt and weld-in connections. In: Klyuev SV (ed) Digital Technologies in Construction Engineering. Springer International Publishing, Cham, pp 321–327

Takai T (2021) Bolt shank shear behavior of high strength bolted frictional joint after slip occurs, focused on unbuttoning. J Struct Eng JSCE (Jpn) 67A:282–295

Wang G, Ding Y (2020) The interface friction in the friction-type bolted joint of steel truss bridge: Case study. Baltic J Road Bridge Eng 15:187–210. https://doi.org/10.7250/bjrbe.2020-15.467

Yamaguchi T, Peng X, Suzuki Y et al (2010) Experimental study on the mechanical behavior of high strength bolted friction type joints with extremely thick plates and many bolts in a line. J Steel Constr Eng (Jpn) 17:23–33

Zhao J, Wang Z, Peng Y et al (2022). Experimental and numerical study on reduction coefficient of the shear capacity of austenitic long stainless-steel bolted connections. https://doi.org/10.1016/j.engstruct.2022.114610

Publisher's Note